Landau Quantization Effects in the Charge-Density-Wave System $(Per)_2M(mnt)_2$ (where M = Au and Pt)

R. D. McDonald,[1] N. Harrison,[1] J. Singleton,[1] A. Bangura,[2] P. A. Goddard,[1] A. P. Ramirez,[3] and X. Chi[3]

[1]*National High Magnetic Field Laboratory, LANL, MS-E536, Los Alamos, New Mexico 87545, USA*

[2]*The Clarendon Laboratory, Parks Road, Oxford OX1 3PU, United Kingdom*

[3]*Bell Laboratories, Lucent Technologies, 600 Mountain Avenue, Murray Hill, New Jersey 07974, USA*

(Received 20 September 2004; published 18 March 2005)

A finite transfer integral t_a orthogonal to the conducting chains of a highly one-dimensional metal gives rise to empty and filled bands that simulate an indirect-gap semiconductor upon formation of a charge-density wave (CDW). In contrast to semiconductors such as Ge and Si with band gaps $\sim$1 eV, the CDW system possesses an indirect gap with a greatly reduced energy scale, enabling moderate laboratory magnetic fields to have a major effect. The consequent variation of the thermodynamic gap with magnetic field due to Zeeman splitting and Landau quantization enables the electronic band structure parameters (transfer integrals, Fermi velocity) to be determined accurately. These parameters reveal the orbital quantization limit to be reached at $\sim$20 T in $(Per)_2M(mnt)_2$ salts, making them highly unlikely candidates for a recently proposed cascade of field-induced CDW states.

DOI: 10.1103/PhysRevLett.94.106404 PACS numbers: 71.45.Lr, 71.20.Rv, 71.70.Di

Magnetic fields B affect the energies of band electrons via Landau (orbital) quantization and Zeeman (spin) splitting [1]. In semiconductors such as GaAs and Si, the characteristic energies of these effects for $B \lesssim 100$ T are much smaller than the energy gap, E_g, and the conduction and valence bandwidths, all of which are $\sim$1 eV; hence, the field can be regarded as a mere perturbation of the overall band structure. By contrast, commensurate charge-density wave (CDW) ground states have the potential to provide analogues in which E_g and the bandwidths are scaled down by factors of $\sim$10–1000 [2]. An ''indirect-gap semiconductor'' is produced in a CDW if the characteristic bandwidth $4t_a$ of the electronic dispersion orthogonal to the chain direction (and nesting vector $\mathbf{Q}$) is comparable to but smaller than the order parameter 2Δ [see Fig. 1(b)]. In such circumstances, the small size of E_g means that the Landau and Zeeman energies due to typical laboratory fields are major effects, resulting in marked alterations to the overall electronic properties.

In this Letter, we show that the CDW materials $(Per)_2M(mnt)_2$, with M = Au and Pt, are ideal candidates for this purpose [3]. Fields of $B < 45$ T have been shown to suppress the CDW ground states of these systems [4–7], providing an estimate for 2Δ of a few meV, only slightly larger than the $4t_a \sim 1.2$ meV obtained from band structure calculations [8]. Landau quantization and Zeeman splitting of the filled and empty states [Fig. 1(d)] lead to a field-dependent thermodynamic energy gap $E_g(B)$ that may, with care, be extracted from the thermally activated component of the conductivity

$$\sigma_T = \sigma_0 \exp[-E_g(B)/2k_B T], \quad (1)$$

where T is the temperature. The measured $E_g(B)$ provides a means of deducing both $4t_a$ and the Fermi velocity $\mathbf{v}_F$ along the chains. These values are consistent with band structure calculations [8] and are in good agreement with estimates from thermopower data [3]. The data also enable us to identify the maximum field at which closed orbits can exist, which is found to be too small to support recently postulated field-induced CDW states in $(Per)_2M(mnt)_2$ salts [6].

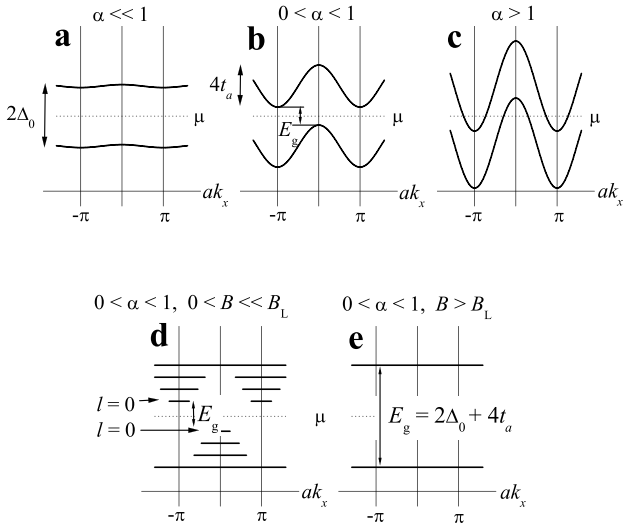

FIG. 1. Electronic dispersion at $k_y' = 0$ according to Eq. (5) for differing values of $\alpha = 2t_a/\Delta$: (a) $\alpha \ll 1$, (b) $0 < \alpha < 1$, (c) $\alpha > 1$. Scenario (b) corresponds to an indirect-gap semiconductor. (d) Schematic of the Landau quantization of scenario (b) in the presence of finite B (ignoring the Zeeman effect, for clarity). (e) The gap beyond the field limit for Landau quantization ($B > B_L$; see text). In all diagrams, μ represents the chemical potential.

Charge transfer between $(\mathrm{Per})_2^+$ and $M(\mathrm{mnt})_2^-$ in $(\mathrm{Per})_2M(\mathrm{mnt})_2$ gives rise to a normal metallic state with four highly one-dimensional (1D) 3/4-filled bands in which $\mathbf{v}_\mathrm{F}$ is directed along the Perylene chains parallel to the crystallographic **b** axis [8]. Near-commensurate CDW ground states occur for $M =$ Pt, Cu, and Au, in which the 1D band becomes gapped upon modulation of the lattice at a postulated [9] wave vector $\mathbf{Q} = (0, 2k_\mathrm{F}, 0)$, where $\pm k_\mathrm{F} \approx \frac{\pi}{4}|\mathbf{b}|$ [10]. Transitions into the CDW ground state occur at $T_\mathrm{P} \approx 12$ K for $M =$ Au and $T_\mathrm{P} \approx 8$ K for $M =$ Pt. In the case of $M =$ Pt, this is accompanied by the synchronous dimerization of the $S = 1/2$ Pt spins [10]: we return to the special case of $M =$ Pt below. In all cases, semiconducting behavior occurs for $T \leq T_\mathrm{P}$; as T is reduced further, in addition to the thermally activated conduction, there is an increasing contribution from the sliding collective mode of the CDW as a characteristic threshold electric field $\mathcal{E}_\mathrm{t}$ is approached [5].

In these experiments, $E_\mathrm{g}(B)$ is determined for $M =$ Au and Pt using transport measurements in static fields of up to 33 T, with $0.45 \leq T \leq 4.2$ K provided by a ^{3}He cryostat. Currents as low as $I = 50$ nA (equivalent to a current density $j_y \sim 50\ \mathrm{A\,m^{-2}}$) applied along the crystal's b direction enable E_g to be extracted from the T dependence of the resistance R (proportional to the resistivity tensor component ρ_{yy} [7]) over a range of T where the contribution from the CDW collective mode is small. Figure 2 shows that this is the case over a wide range of B provided $I \lesssim 100$ nA and $T \gtrsim 1$ K.

Figures 3(a) and 3(b) show examples of Arrhenius plots of the resistance R versus $1/T$ for $M =$ Au and Pt, respectively, made using $I = 50$ nA with $\mathbf{B}||\mathbf{c}^*$ at several different B. Prior studies revealed ρ_{yy} in $(\mathrm{Per})_2M(\mathrm{mnt})_2$ [5,7] to be consistent with a scenario in which $\sigma_{xy} \approx 0$. Hence,

$$\rho_{yy} \approx (\sigma_T + j_y/\mathcal{E}_\mathrm{t})^{-1}, \tag{2}$$

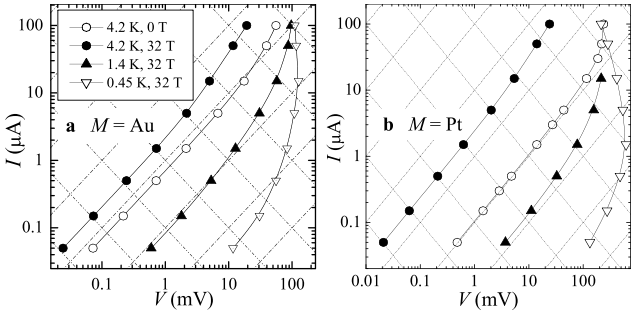

FIG. 2. Nonlinear current-versus-voltage characteristics of (a) $(\mathrm{Per})_2\mathrm{Au}(\mathrm{mnt})_2$ and (b) $(\mathrm{Per})_2\mathrm{Pt}(\mathrm{mnt})_2$ plotted on logarithmic scales for various temperatures and fields (see inset key). The negative-slope diagonal lines are contours of constant power, and the positive-slope diagonal lines are contours of constant resistance, providing a guide as to when the sample's behavior is dominated by Ohmic, thermally activated conduction rather than sliding.

where $j_y/\mathcal{E}_\mathrm{t}$ is the contribution from the collective mode. As discussed below, the expression for $E_\mathrm{g}(B)$ [Eq. (7)] contains Δ, which is T dependent; moreover, $\mathcal{E}_\mathrm{t}$ may depend on T. Thus, the slope of an Arrhenius plot becomes

$$\frac{\partial \ln\rho_{yy}}{\partial(1/T)} \approx \frac{\frac{1}{2k_\mathrm{B}}(E_\mathrm{g} - T\frac{\partial E_\mathrm{g}}{\partial T}) - \frac{j_y T^2}{\sigma_T \mathcal{E}_\mathrm{t}^2}\frac{\partial \mathcal{E}_\mathrm{t}}{\partial T}}{1 + \frac{j_y}{\sigma_T \mathcal{E}_\mathrm{t}}}. \tag{3}$$

Since $\mathcal{E}_\mathrm{t}$ is expected to depend strongly on T only as $T \rightarrow T_\mathrm{P}$ [11], the last term on the right-hand side of Eq. (3) should be negligible for $T \lesssim T_\mathrm{P}/2$ and sufficiently small j_y. The second term can also be minimized by evaluating the slope for $T < T_\mathrm{P}/2$; using a mean-field expression for $\Delta(T)$ [2], these conditions give $-2T\partial E_\mathrm{g}/\partial T \equiv -T\partial\Delta/\partial T < 0.1\Delta$. In the present case, we choose $T \approx T_\mathrm{P}/3$, such that $-T\partial\Delta/\partial T \approx 0.05\Delta$, yielding $\partial\ln(\rho_{yy})/\partial(1/T) \approx E_\mathrm{g}/2k_\mathrm{B}$ with a systematic error of only $\sim$5%. In using this method to extract E_g, it is important to note that $T_\mathrm{P} = T_\mathrm{P}(B)$ [4]; thus, the exact T range used depends on the applied field.

At lower T, the number of thermally activated carriers decreases significantly, rendering their contribution to the conductivity negligible. The consequent larger potential difference across the sample results in increased depinning of the CDW, so that $\ln(R)$ saturates at lower T (i.e., higher $1/T$) in Fig. 3. As shown in Fig. 2, the point at which significant CDW depinning occurs is shifted to lower T (higher $1/T$) by the use of small currents.

Using larger currents of 1 and 10 μA, Graf *et al.* [4] obtained an Arrhenius plot in which the CDW was highly depinned over an extensive range of T, causing $\ln(\rho_{yy})$ versus $1/T$ to exhibit significant curvature even at $T \sim T_\mathrm{P}/3$. To make matters worse, Graf *et al.* extracted $\partial\rho_{yy}/\partial(1/T)$ at $T \approx 0.7T_\mathrm{P}$, at which $-T\partial\Delta/\partial T > \Delta$. Sadly, these factors resulted in an overestimate of E_g by a factor of $\sim$2.

The present estimate of $E_\mathrm{g} \approx 3.2$ meV made at $T \approx T_\mathrm{p}/3$ and $B = 0$ with $I = 50$ nA, shown in Fig. 4(a), is rather less than the value of $2\Delta_0 \approx 4.5$ meV deduced for

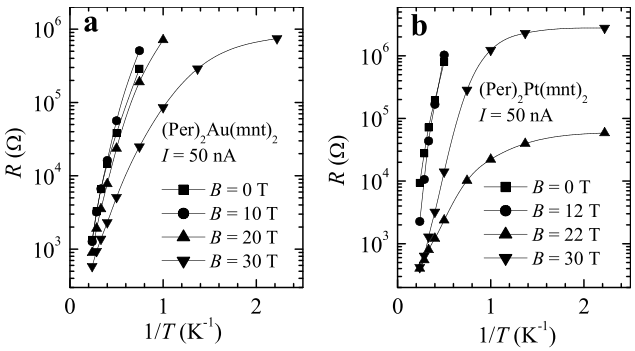

FIG. 3. Arrhenius plots of R (logarithmic scale) versus $1/T$ with $I = 50$ nA for (a) $M =$ Au and (b) $M =$ Pt at several different magnetic field strengths B.

M = Au from its Pauli paramagnetic limit [5], supporting the scenario depicted in Fig. 1(b). This can be modeled using a simplified dispersion of the form

$$\varepsilon = -2t_a \cos ak_x - \hbar v_F |k_y - k_F|, \quad (4)$$

where $v_F = \sqrt{2}bt_b/\hbar$ is the magnitude of $\mathbf{v}_F$ directed along $\mathbf{b}$ for a $\frac{3}{4}$-filled band. Here, t_a, t_b, $a(\approx 17\,\text{Å})$, and $b(\approx 4.2\,\text{Å})$ are the transfer integrals and lattice spacings perpendicular and parallel to the chains, respectively. On opening a gap 2Δ (which may be smaller than $2\Delta_0$ at finite T), the dispersion becomes [11]

$$\varepsilon_g = -2t_a \cos ak_x \pm \sqrt{(\hbar v_F k_y')^2 + \Delta^2}, \quad (5)$$

where we have substituted $k_y' = k_y - k_F$ for clarity. At $k_y' = 0$, the electronic dispersion versus k_x consists of a pair of narrow bands above and below μ, separated in energy by 2Δ, as shown in Fig. 1 for different values of $\alpha = 2t_a/\Delta$. When $\alpha \ll 1$, one obtains a gap with little dispersion. This is the likely scenario for CDW materials with very large order parameters such as $(TaSe_4)_2I$ or TaS_3 [2]. In the opposite extreme, $\alpha > 1$, one obtains a semimetal qualitatively similar to $NbSe_3$ [2] or perhaps α-(BEDT-TTF)$_2M$Hg(SCN)$_2$, in which field-induced CDW phases have been suggested [12]. An indirect-gap semiconductor with $E_g = 2\Delta - 4t_a$ between filled and empty states separated by the vector $[\pi/a, 0]$ is obtained for the intermediate situation where $0 < \alpha < 1$.

The introduction of finite B has two effects on Eq. (5). The first is to Zeeman split the two bands into four subbands with energies

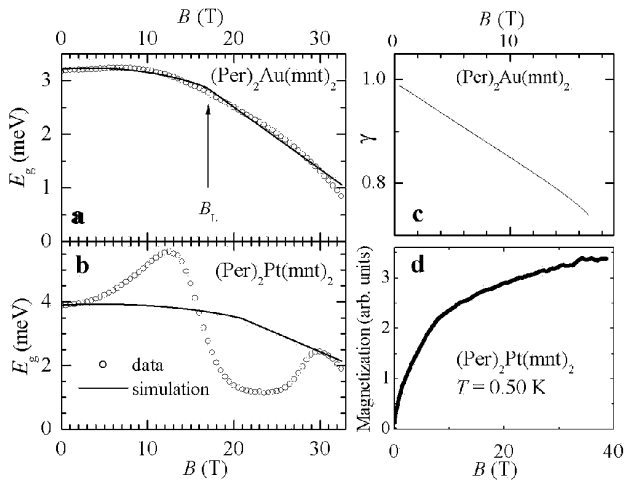

FIG. 4. The excitation gap E_g (circles) for (a) M = Au and (b) M = Pt estimated from the slopes of Arrhenius plots like those in Fig. 3 at $T \approx T_P/3$ at many different values of the applied B. The solid lines represent fits of the model described in the text. (c) The parameter $\gamma(B)$ obtained by fitting the experimentally estimated gap in (a). (d) Magnetization of many randomly orientated M = Pt crystals at $T = 0.50$ K measured using an extraction magnetometer in a pulsed magnetic field [15].

$$\varepsilon_g = -2t_a \cos ak_x \pm \sqrt{(\hbar v_F k_y')^2 + \Delta^2} + gs\mu_B B, \quad (6)$$

where s $(= \pm\frac{1}{2})$ is the electron spin and g (≈ 2) is its Landé g factor. Thus, the smallest (*thermodynamic*) gap occurs between the maximum of the $s = +\frac{1}{2}$ subband below μ and the minimum of the $s = -\frac{1}{2}$ subband above μ, yielding $E_g = 2\Delta - 4t_a - g\mu_B B$. The second effect of finite B is to quantize the orbital motion of the empty and filled states immediately above and below the gap, giving rise to sets of completely empty and filled Landau levels at $T = 0$ [Fig. 1(d)]. At finite T, carrier excitations occur between the $l = 0$ Landau levels on either side of μ, leading to a thermodynamic gap

$$E_g(B) = 2\Delta - 4t_a - g\mu_B B + \gamma\hbar\omega_c, \quad (7)$$

where $\omega_c = eB/m^*$ is the magnitude of the cyclotron frequency of the $l = 0$ Landau level of the two relevant subbands in the limit $B \to 0$ and m^* is an effective mass, to be defined below.

The parameter γ (where $\gamma \to 1$ as $B \to 0$) is introduced to account for the (identical) nonparabolicities of the $s = +\frac{1}{2}$ subband below μ and the $s = -\frac{1}{2}$ subband above μ; its field dependence is obtained by equating the k-space area $A_k(\varepsilon_g)$ of an orbit of constant energy ε_g [from Eq. (6)] with the Onsager k-space area $A_{l=0} = \pi eB/\hbar$ of the $l = 0$ Landau level [1]. This cannot be done analytically; instead, the fit (solid line) to the data in Fig. 4(a) for M = Au incorporates a numerical integration $A_k(\varepsilon_g) = \int \Theta|\varepsilon_g| dk_x dk_y'$, where Θ is the theta function (i.e., the integral of the Kronecker δ).

The fit involves adjusting three parameters, $2\Delta + 4t_a$, $4t_a$, and v_F. A satisfactory fit is obtained for M = Au using $2\Delta + 4t_a = 4.81 \pm 0.03$ meV, $4t_a = 0.80 \pm 0.03$ meV, and $v_F = (1.70 \pm 0.05) \times 10^5$ ms^{-1}, so that $2\Delta = 4.02 \pm 0.04$ meV; note that over the T range used, the deduced value of Δ is equal to Δ_0 to a good approximation. These parameters correspond to $E_g = 3.21 \pm 0.07$ meV at $B = 0$, $T = 0$ and transfer integrals $t_a \approx 0.2$ meV and $t_b \approx 188$ meV; the latter is close to estimates from thermopower data ($t_b \approx 185$ meV) [3]. Moreover, both transfer integrals are in reasonable accord with band structure calculations, which yield $149 < t_b < 354$ meV, the computed value depending on the number of basis sets, and $t_a \approx 0.3$ meV [8].

Figure 4(c) shows the field dependence of γ in Eq. (7). At $B = 0$, $\gamma = 1$ due to the approximately parabolic curvature of the bands close to their extrema

$$\varepsilon_g \approx 2\Delta - 4t_a \pm g\mu_B B + \frac{\hbar^2 k_x^2}{2m_a} + \frac{\hbar^2 k_y'^2}{2m_\Delta} + \ldots. \quad (8)$$

Here, $m^* = 0.90m_e$ is an effective mass (m_e is the free electron mass), given by $m^* = \sqrt{m_a m_\Delta}$ for an approximately elliptical orbit where $m_a = \hbar^2/2a^2t_a \approx 50m_e$ and $m_\Delta = \Delta/v_F^2 \approx 0.01m_e$. Equation (7) therefore describes a situation in which E_g initially increases with B at a rate

$\partial E_g/\partial B \approx \hbar e(m_e - m^*)/m^* m_e$, owing to the fact that $m^* < m_e$ and $g\mu_B \approx \hbar e/m_e$. As B increases further, the nonparabolic curvature of Eq. (6) at $|\varepsilon_g| > \Delta - 2t_a - gs\mu_B B$ eventually causes E_g to fall, corresponding to a reduction in γ in Fig. 4 (inset). This occurs until the $l = 0$ Landau level of each subband acquires an energy of magnitude $|\varepsilon_g(B)| = |(\Delta + 2t_a - gs\mu_B B_L)|$ at the limit

$$B_L = 8t_a m^*/\gamma\hbar e, \tag{9}$$

at which $\gamma\hbar\omega_c = 8t_a$, $k_x = \pi/a$ and closed orbits can no longer exist. This limit corresponds to the largest possible pocket created by imperfect nesting matching the k-space area $A_{l=0} \approx 10^{17}$ m^{-2} ($\approx 0.15\%$ of the Brillouin zone) of the $l = 0$ Landau level. Orbitally quantized states therefore cannot exist in $(Per)_2Au(mnt)_2$ at $B > 17$ T, supporting the existence of an inhomogeneous CDW phase in this material at $B \gtrsim 30$ T [7] as opposed to a cascade of field-induced CDW states involving orbital quantization [12,13]. The absence of Landau subbands for $B \geq B_L \approx 17$ T ($M =$ Au) leads to a simpler field-dependent gap

$$E_g = 2\Delta + 4t_a - g\mu_B B. \tag{10}$$

The slope for $B > B_L$ is determined entirely by $|gs| \approx 1$, making it independent of all fitting parameters. Only the intercept of Eq. (10) at $B = 0$ is determined by $2\Delta + 4t_a$. Hence, the portion of the fit for $B > B_L$ in Fig. 4(a) effectively involves the adjustment of only a single parameter, imposing a severe contraint on $2\Delta + 4t_a$ and thereby adding further confidence in the model.

For $M =$ Au, we have shown that a uniform CDW order parameter $2\Delta_0 \approx 2\Delta = 4.02 \pm 0.04$ meV, bandwidth $4t_a = 0.80 \pm 0.03$ meV, and Fermi velocity $v_F = (1.70 \pm 0.05) \times 10^5$ ms^{-1} explain the observed field dependence of E_g. This requires a revision of our estimate for the Pauli paramagnetic limit to $B_P = (\Delta_0 + 2t_a)/\sqrt{2}gs\mu_B \approx 30$ T, which now approximately corresponds to the field at which $\mathcal{E}_t$ starts to drop experimentally [5]. The revised estimate of $2\Delta_0$ further yields $\zeta = k_B T_P/2\Delta_0 \approx 3.9$: since this estimate only slightly exceeds the BCS value $\zeta = 3.52$, it implies that the CDW ground state of $(Per)_2M(mnt)_2$ with $M =$ Au is weakly coupled to the crystalline lattice [2].

Turning now to the case of $M =$ Pt, it is clear that E_g is larger at $B = 0$, in spite of the lower T_p (≈ 8 K). The complex field-dependent behavior that takes place for $3 < B < 30$ T only in the case of $M =$ Pt must be the consequence of interactions involving the dimerization of the $S = 1/2$ Pt spins, which are not included in the present simulation. In situations in which the magnetization [Fig. 4(d)] is either small ($B \approx 0$) or approaching saturation ($B \approx 30$ T), the use of $4t_a = 1$ meV and the same v_F as in $M =$ Au results in a fitted value $2\Delta \approx 4.8$ meV. In the absence of a more sophisticated model, one can conclude from the estimate of $\zeta = 2\Delta_0/k_B T_P \approx 7$, that the dimerization of the Pt spins in $(Per)_2Pt(mnt)_2$ causes the CDW ground state to be more strongly coupled to the crystalline lattice than in the case of $M =$ Au. The consequent larger lattice distortion in $M =$ Pt might explain its higher $\mathcal{E}_t$ values compared to those of $M =$ Au (Fig. 2). It may also be the reason why x-ray Bragg reflection peaks due to dimerization have been seen for $M =$ Pt but not for $M =$ Au [3].

In conclusion, $(Per)_2Au(mnt)_2$ is shown to possess an ideal combination of parameters for modeling the effect of a strong magnetic field on an indirect-gap semiconductor. A model that includes the effect of Zeeman splitting and Landau quantization of subbands with a conventional field-independent order parameter (for fields below the Pauli paramagnetic limit) provides a good description of the experimental data [14]. The electronic structure parameters obtained reveal the limiting magnetic field for closed orbits to be $B_L \approx 17$ T, implying field-induced CDW states that incorporate orbitally quantized levels cannot exist at $B \gtrsim 17$ T in $(Per)_2Au(mnt)_2$. The electronic structure of $(Per)_2Pt(mnt)_2$ is expected to be similar. However, the existence of $S = 1/2$ Pt spins causes a stronger coupling of the CDW to the lattice followed by a more complex dependence of E_g on field for $B \lesssim 30$ T that has yet to be modeled.

This work is supported by U.S. Department of Energy (DOE) Grants No. LDRD20030084DR and No. LDRD2004009ER and was performed under the auspices of the National Science Foundation, the DOE, and the State of Florida.

[1] N. W. Ashcroft and N. D. Mermin, *Solid State Physics* (Saunders College Publishing, Philadelphia, 1976).
[2] G. Grüner, *Density Waves in Solids*, Frontiers in Physics Vol. 89 (Addison-Wesley, Reading, MA, 1994).
[3] R. T. Henriques *et al.*, J. Phys. C **17**, 5197 (1984).
[4] D. Graf *et al.*, Phys. Rev. B **69**, 125113 (2004).
[5] R. D. McDonald *et al.*, Phys. Rev. Lett. **93**, 076405 (2004).
[6] D. Graf *et al.*, Phys. Rev. Lett. **93**, 076406 (2004).
[7] R. D. McDonald *et al.*, cond-mat/0408408.
[8] E. Canadell *et al.*, cond-mat/0411676; Europhys. B (to be published).Typical widths of the dispersion parallel to the a axis are ≈ 1.2 meV, which can be parametrized by an effective transfer integral $t_a \approx 0.3$ meV. The $2\delta \sim 4$ meV splitting of the four bands into two sets of quasidegenerate bands suggests the possibility of two coexisting nesting vectors $\mathbf{Q} \pm (0, 2\delta/\hbar v_F, 0)$, which, by symmetry arguments, should give approximately the same Δ and E_g for each pair of bands.
[9] V. Gama *et al.*, Synth. Met. **56**, 1677 (1993).
[10] E. B. Lopes *et al.*, J. Phys. I (France) **6**, 2141 (1996).
[11] B. Korin-Hamzić *et al.*, Europhys. Lett. **59**, 298 (2002).
[12] D. Andres *et al.*, Phys. Rev. B **68**, 201101 (2003).
[13] A. G. Lebed, JETP Lett. **78**, 138 (2003).
[14] A similar model has been applied successfully to the spin-density-wave state of $(TMTSF)_2PF_6$, for which Zeeman effects are absent [11]. We are grateful to Kazumi Maki for pointing this work out to us.
[15] P. A. Goddard *et al.* (to be published).